RSC Advances

This article can be cited before page numbers have been issued, to do this please use: J. Li, Y. Yao, L. Yuan, Z. Zhang and F. zhang, *RSC Adv.*, 2016, DOI: 10.1039/C6RA05682B.

ROYAL SOCIETY OF CHEMISTRY

www.rsc.org/advances

View Article Online
DOI: 10.1039/C6RA05682B

Novel porphyrin-Schiff base conjugates: synthesis, characterization and in vitro photodynamic activities

Ya-Hong Yao[a,b], Jun Li[a,*], Long-Fei Yuan[a], Zeng-Qi Zhang[a] and Feng-Xing Zhang[a]

[a)] Key Laboratory of Synthetic and Natural Functional Molecule Chemistry of Ministry of Education, College of Chemistry & Materials Science, Northwest University, Xi'an, Shaanxi 710069, China)

[b)] College of Science, Xi'an University of Architecture and Technology, Xi'an, Shaanxi 710055, China

*corresponding author, e-mail: junli@nwu.edu.cn

Abstract

Three novel porphyrin-Schiff base conjugates derived, namely, tetra[4-(4-hydroxy benzylideneamino)] phenyl porphyrin (**3a**), tetra[4-(2-thienyldeneamino)]phenyl porphyrin **(3b)** and tetra [4-(2-pyridyldeneamino)]phenyl porphyrin **(3c)** from the tetra (4-aminophenyl) porphyrin (**TAPP)** were synthesized and characterized by IR, UV-vis, ^{1}H NMR, HRMS and elementary analysis. Their biological activities against human epidermoid carcinoma (A431) cells were evaluated with a MTT assay. As we expected, the porphyrin conjugates showed negligible cytotoxicity to A431 cells in the absence of light. While their phototoxic activities were improved after irradiated with LED lamp (425nm) and increased significantly with the increase of doses. The fluorescence microscope pictures revealed that three porphyrin-Schiff conjugates could diffuse into skin cancer cells, demonstrating that these compounds are potential candidates for photodynamic therapy agents.

Keywords: Porphyrin; Schiff base; Anti-tumor activity; Photodynamic therapy; Cytotoxicity

View Article Online
DOI: 10.1039/C6RA05682B

1. Introduction

Cancer is one of the deadliest diseases of in nowadays. The traditional cancer treatments, including surgery, chemotherapy and radiation therapy, may cause serious side effects resulted from the loss of normal organ function [1, 2]. In contrast, photodynamic therapy (PDT) can selectively destroy malignant cells by the administration of a non-toxic photosensitizer and hold the potential for minimal side effects [3, 4]. Upon irradiation with light of specific wavelength, photosensitizer transfers energy to triplet oxygen ($^3O_2$), and then generates singlet oxygen ($^1O_2$) and other reactive oxygen species (ROS) near the tumor. These generated molecules can cause intracellular oxidative damages and cell death through apoptosis or necrosis [5, 6].

Porphyrins and their derivatives, as a promising photosensitizer, have attracted extensive attention in the field of PDT for cancer treatment [7-10]. This is due to the obvious advantages of porphyrins, such as favourable wavelength, intense absorption in visible region of the electromagnetic spectrum and low intrinsic toxicity [11]. Moreover, it has been demonstrated that porphyrins prefer to accumulate in tumor cells in vitro and in vivo rather than in normal tissue. Notably the first-generation photosensitizer Photofrin is a complex mixture of hematoporphyrins derivatives and has been approved by the United States Food and Drug Administration (FDA) for PDT treatment of various cancers such as oesophageal cancer, early-and late-stage lung cancer, bladder cancer and malignant, nonmalignant and early-stage cervical cancer [12-14]. There has been a growing interest in the synthesis and functionalization of porphyrins for the chemists [15, 16].

Schiff bases were an important class of organic compounds, and were reported to have a wide range of biological activities including antiviral, anticancer, cytotoxic, antimicrobial, etc. [17, 18]. Thus, development and synthesis of novel Schiff base derivatives as potential chemotherapeutics attracted the attention of organic and medicinal chemists [19]. Furthermore, hydroxyl group endows compounds good solubility in aqueous environment, and is a commonly used hydrophilic moiety in dissolution of some photosensitizers. Thereby porphyrin conjugate with hydroxyl groups was expected to enhance its therapeutic efficacy in vitro [20-22]. Besides,

View Article Online
DOI: 10.1039/C6RA05682B

heterocyclic rings such as thiophene, furan and pyrrole in the compounds, have played a major role in expanding their pharmacological properties. For example, pregnenolone derivatives containing heterocyclic moieties were found to exhibit anticancer activity [23, 24]. In addition, suitable candidates for photosensitizer were obtained by attaching various substituents to the peripheral positions of the porphyrin core.

Herein, we reported the design and synthesis of the porphyrin-Schiff base conjugates, which bearing hydroxyl groups, thienyl and pyridyl groups on porphyrin peripheral substituents positions **3a-3c (Sheme 1)**. In addition, we evaluated their cytotoxic activity against human skin cancer cell lines and normal skin cells. Furthermore, the photodynamic therapy and cellular uptake of the porphyrins in the tumor cells are also investigated.

2. Experimental

2.1 Materials and Instruments

^{1}H-NMR spectra were collected in a Varian Inova 400 MHz NMR spectrometer. Deuterated dimethylsulfoxide (d_6-DMSO) was used as solvent and TMS as internal reference. Elemental analyses (C, H and N) were performed on a Vario EL-III CHNOS instrument. Mass spectra (MS) were recorded on a matrix assisted laser desorption/ionization time of flight mass spectrometer (MALDI-TOF MS, Krato Analytical Company of Shimadzu Biotech, Manchester, Britain). FT-IR (4000-400 cm^{-1}) spectra were obtained with samples in KBr matrix for the title complexes on A BEQUZNDX-550 series FT-IR spectrophotometer. The UV-vis spectra were recorded on a Shimadzu UV1800 UV-vis-NIR spectrophotometer using $CHCl_3$ as solvent. Fluorescence spectra were recorded in $CHCl_3$ with a HITACHI F-4500 spectrophotometer. Chromatographic purification was performed with silica gel (100–120 mesh). 3-(4, 5-dimethylthiazol-2-yl)-2, 5-diphenyl tetrazolium bromide (MTT) were purchased from Sigma-Aldrich Japan (Chiba, Japan). Pyrrole and DMF were distilled before use. All the other solvents and reagents were used without further purification.

View Article Online
DOI: 10.1039/C6RA05682B

2.2 Synthesis of porphyrins

2.2.1 Tetra (4-nitrophenyl) porphyrin (TNPP)

The synthetic method of TNPP was presented in the previous report [25, 26], as shown in Scheme 1. In the 250 mL three-necked flask, *p*-nitrobenzaldehyde (5.5 g, 36 mmol) and acetic anhydride (6 mL, 64 mmol) were added to a refluxing mixture of propionic acid (150 mL), then freshly distilled pyrrole (2.5 mL, 36 mmol) in 10 mL of propionic acid was dropwise added (ca. 30 min) to the mixture with stirring. The reaction mixture was brought to reflux for 2 h. The mixture was allowed to cool overnight for efficient precipitation, and a dark residue was collected by filtration. The dark solid was washed with water and dried in vacuum. The solid was purified in 40 mL of refluxing pyridine for 1 h. After that, the solution was cooled to room temperature and stored at -4 ºC overnight. Then the mixture was filtered under vacuum and washed with acetone till the eluent became colorless. The yield of the purified red brown product was 12%.

*2.2.2 Tetra (4-aminophenyl) porphyrin (**TAPP**)*

The above obtained TNPP (1.5 g, 1.9 mmol) was dissolved in 75 mL of concentrated HCl solution, and the aqueous solution was heated to 75~80 ºC in a water bath. Then another concentrated HCl solution (25 mL) with $SnCl_2 \cdot 2H_2O$ (10.0 g, 44 mmol) was added slowly into the aforementioned solution under stirring, and followed by heating to 75~80 ºC for 2 h. After finishing the heating treatment, the reaction mixture was cooled with a cold-water bath and then an ice bath, and neutralized to weak base by adding concentrated $NH_3 \cdot H_2O$ slowly. Then solid was collected by filtration, and mixed vigorously with 5% NaOH (150 mL). The mixture was filtered and washed with distilled water repeatedly. The residue was extracted by Soxhlet extraction with 200 mL of chloroform and then removed the solvent under vacuum. The crude product was purified by SiO_2 column chromatography (CH_2Cl_2/EtOH=2:1) to give purple porphyrin **TAPP**. Yield: 30.0%. M.p. >250 ºC; Anal. Calcd. for $C_{44}H_{34}N_8$(%): C, 78.32; H, 5.08; N, 16.60. Found: C, 77.89; H, 5.14; N, 16.27. MS, m/z : 676.00 $[M+H]^+$amu; UV-vis ($CHCl_3$) λ_{max}: nm 428 (Soret band),

View Article Online
DOI: 10.1039/C6RA05682B

523 (Q_I), 563 (Q_{II}), 604 (Q_{III}), 655 (Q_{IV}); IR (KBr)/cm^{-1}: 3443 ($\nu_{vs\ N-H}$, amino), 3375 (ν_{N-H}, pyrrole), 1512 (δ_{N-H}, amino), 1465 ($\nu_{C=N}$, pyrrole), 1288 (ν_{C-N}, amino). ^{1}H NMR (d_6-DMSO, 300 MHz): H, ppm 8.89 (s, 8H, β position of the pyrrole moiety), 7.86 (d, 8H, ArH), 7.01 (d, 8H, ArH), 5.58 (s, 8H, amine), -2.74 (s, 2H, innerNH).

*2.2.3 General procedure for the synthesis of the porphyrin-Schiff base conjugates **3a–3c***

TAPP (0.2 g, 0.2959 mmol), dissolved in 20 mL of anhydrous ethanol, was heated to reflux, and another ethanol solution (30 mL) with aldehyde (9 mmol) was added dropwise into the solution, followed by refluxing the mixture for 3 h. The process of the reaction was monitored by TLC. After finishing the reaction, the mixture was fully cooled down and the precipitate was filtered off and washed with ethanol repeatedly. The solid was dried under vacuum. The obtained violet product was dissolved in dichloromethane, and purified by column chromatography (the silica gel column was pretreated with alkaline triethylamine to prevent the dissociation of the product) using a binary eluent of dichloromethane and ethanol.

*Tetra [p-(p-hydroxy benzylideneamino)] phenyl porphyrin（**3a**）*

The compound **3a** was prepared from compound **TAPP** (0.2 g, 0.2959 mmol), and *p*-hydroxybenzaldehyde (1.1 g, 9 mmol) according to the above given procedure. Yield 72%. M. p. >250 ºC; Anal. Calcd. for $C_{72}H_{50}N_8O_4$(%): C, 79.25; H, 4.62; N, 10.27. Found: C, 78.91; H, 4.27; N, 9.91. MALDI-TOF-MS: m/z 1091.4018 for $[M+1]^+$ (calcd 1091.3955); UV-vis ($CHCl_3$) λ_{max}: nm 426 (Soret band), 521 (Q_I), 559 (Q_{II}), 603 (Q_{III}), 654 (Q_{IV}); IR (KBr)/cm^{-1}: 3314 (ν_{N-H}, pyrrole), 3423 (ν_{O-H}, phenyl), 1580 ($\nu_{C=N}$, Schiff base), 1512 ($\nu_{C=C}$, phenyl), 1159 (δ_{C-N}, pyrrole). ^{1}H NMR (d_6-DMSO, 300 MHz): H, ppm 10.22 (s, 4H, -OH), 8.92 (s, 8H, β position of the pyrrole moiety), 8.83 (s, 4H, Schiff base), 8.20-8.22 (d, *J*=7.1, 8H, phenyl), 7.94-7.96 (d, *J*=7.1, 8H, phenyl), 7.62-7.64 (d, *J*=7.1, 8H, phenyl), 6.97-6.99 (d, *J*=7.8, 8H, phenyl), -2.83 (s, 2H, inner NH).

*Tetra [p-(2 - thienyldeneamino)] phenyl porphyrin（**3b**）*

The compound **3b** was prepared from compound **TAPP** (0.2 g, 0.2959 mmol), and 2-thenaldehyde (1.0 g, 9 mmol) according to the procesures similar to that of

View Article Online
DOI: 10.1039/C6RA05682B

compound **3a**. Yield 48%. M.p.>250 ºC; Anal. Calcd. for $C_{64}H_{42}N_8S_4$ (%): C, 73.11; H, 4.03; N, 10.66. Found: C, 73.58; H, 3.95; N, 10.28. MALDI-TOF-MS: m/z 1051.4948 for $[M+1]^+$ (calcd 1050.2415); UV-vis ($CHCl_3$) λ_{max}: nm 425 (Soret band), 519 (Q_I), 558 (Q_{II}), 596 (Q_{III}), 651 (Q_{IV}); IR (KBr)/cm^{-1}: 3445 (ν_{N-H}, pyrrole), 1618 ($\nu_{C=N}$, Schiff base), 1585 ($\nu_{C=C}$, phenyl), 1169 (δ_{C-N}, pyrrole), 716 (ν_{C-S}, thienyl). ^{1}H NMR (d_6-DMSO, 300 MHz): H, ppm 9.18 (s, 4H, Schiff base), 8.94 (s, 8H, *β* position of the pyrrole moiety), 8.22-8.26 (d, *J*=7.3, 8H, phenyl), 7.92-7.94 (d, *J*=5.0, 4H, thienyl), 7.85 (s, 4H, thienyl), 7.72-7.74 (d, *J*=7.3, 8H, phenyl), 7.33 (s, 4H, thienyl), -2.84 (s, 2H, inner NH).

*Tetra [p-(2 –Pyridyldeneamino)] phenyl porphyrin（**3c**）*

The compound **3c** was also prepared from compound **TAPP** (0.2 g, 0.2959 mmol), and 2-pyridinecarboxaldehyde (1.0 g, 9 mmol) according to aforementioned procedures. Yield 72%. M.p. >250 ºC; Anal. Calcd. for $C_{68}H_{46}N_{12}$(%): C, 79.20; H, 4.50; N, 16.30. Found: C, 78.97; H, 4.27; N, 16.46. MALDI-TOF-MS: m/z 1032.3773 for $[M+1]^+$ (calcd 1031.1732); UV-vis ($CHCl_3$) λ_{max}: nm 420 (Soret band), 520 (Q_I), 558 (Q_{II}), 596 (Q_{III}), 649 (Q_{IV}); IR (KBr)/cm^{-1}: 3437 (ν_{N-H}, pyrrole), 3053 (ν_{C-H} pyridyl), 1628 ($\nu_{C=N}$, Schiff base), 1569 ($\nu_{C=C}$, phenyl), 1173 (δ_{C-N}, pyrrole), 800 (δ_{C-H}, pyridyl). ^{1}H NMR (d_6-DMSO, 300 MHz): H, ppm 8.93-8.98 (d d, *J*=6.5 *J*=6.2, 8H, *β* position of the pyrrole moiety), 8.83 (s, 4H, Schiff base), 8.31-8.37 (m, 8H, phenyl), 8.03-8.09 (d, *J*=7.5, 4H, pyridyl), 7.88-7.94 (m, 4H, pyridyl), 7.83 (s, 8H, phenyl), 7.72 (t, 4H, pyridyl), 7.63 (t, 4H, pyridyl), -2.83 (s, 2H, inner NH).

2.3 Photodynamic activity experiments in vitro

2.3.1 Cell culture and incubation conditions

The A431cells and human keratinocyte (HaCaT) cells were cultured in a humidified incubator at 37^{o}C with 5% CO_2 in DMEM/F-12 medium supplemented with 10% fetal bovine serum, 100 U/mL penicillin and 100 μg/mL streptomycin. The medium was replaced with fresh cell culture medium every 48 h. When ~80% the confluence was reached, the medium was removed and washed with 5mL of phosphate buffer saline (PBS) for three times, and then cells were replaced with fresh medium for subculture. The porphyrin-Schiff base conjugates were dissolved in

View Article Online
DOI: 10.1039/C6RA05682B

DMSO at a concentration of 5 mM as the stock solution and then diluted with complete medium to the required concentration immediately prior to use. The final DMSO concentration was always below 0.5 % v/v, which showed no effects on cell viability.

*2.3.2 Cellular treatment with porphyrins **3a-3c***

To evaluate the cytotoxicity of compounds **3a-3c** in dark (cytotoxicity without light exposure), cells in the exponential growth phase were seeded at a density of 2×10^4 cells/mL in 96-well culture plates containing a 200 μL culture medium per well. Then cells were incubated for 24 h at 37 ºC to allow for cell adherence. The medium was then replaced with the **3a–3c** solutions in cell culture medium (10 μM) and incubated for 24 h in the dark. Every plate had three wells without complexes as the control and cells treated with each compound was assessed in three copies. HaCaT cells were treated in the same conditions just for comparison. Phototoxicity experiments were performed with A431 cells in 96-well plates similar to the procedures as above described. After then, the compounds solutions were removed, and the cells were washed with 5 mL of PBS for three times and exposed to blue light.

2.3.3 Irradiation

Irradiation was carried out using a blue light source, which was a LED equipped with a 150W lamp. A wavelength range between 400 and 450 nm was selected using optical filters. The light intensity at the treatment site was 100mW/cm^2. Exposure time was 0s and 480s, in which cells were delivered 0 J/cm^2 and 48 J/cm^2.

2.3.4 Determination of cytotoxicity and phototoxicity of the porphyrin-Schiff base conjugates

The determination of cell survival was documented by the MTT assay[27, 28]. Briefly, this method is based on the reduction of MTT to a coloured formazan compound (λ_{max}=570 nm) by the active mitochondrial hydrogenase in living cells. After 24 h incubation with each compound, 20 μL MTT (5 mg/mL) in PBS was added to each well and incubated for another 4 h in a humidified incubator with 5% CO_2 at 37 °C. The MTT solution was then removed and 150 μL DMSO was added to each well to lyse the released formazan dye. The data were recorded by optical density (OD) at

View Article Online
DOI: 10.1039/C6RA05682B

570 nm. The relative cell viability was expressed as the OD absorbance of tested compound versus that of the control. The same procedures were carried out without irradiation to determine the toxicity of normal skin cells in dark.

2.4 **Cellular uptake of porphyrin conjugates**

The HaCaT and A431 cells were seeded on 24-well culture plates in complete culture medium and allowed to adhere for overnight. The porphyrin-Schiff base conjugates (10 μM) were added to each well and incubated at 37 °C in the dark for 24 h, followed by washing twice with PBS. The cellular uptake of porphyrin-Schiff base conjugates was examined under fluorescence microscopy with a filter set at 535 nm excitation light (BP 515–560, FT 580, LP 590).

3. Results and discussion

3.1. Synthesis of porphyrin-Schiff base conjugates

Three novel porphyrin-Schiff conjugates **3a-3c** were successfully synthesized according to the synthetic route in **Scheme 1** and characterized by elemental analysis, mass spectroscopy, UV-vis spectroscopy and ^{1}H NMR spectroscopy. In order to get the target porphyrin-Schiff base conjugates, TNPP was firstly obtained through the reaction of pyrrole and *p*-nitrobenzaldehyde with the molar ratio of 1:1 under refluxing propionic acid by Adler's strategy. Then TNPP was reduced by $SnCl_2 \cdot 2H_2O$ in concentrated HCl solution to get the key intermediate **TAPP**. Finally, the three conjugates were obtained from condensation of amine groups of **TAPP** with different aldehydes in a mixture of dichloromethane and ethanol under reflux. The formation of C=N bond can be greatly accelerated by addition of anhydrous magnesium sulfate to the solution, which improved the yields of conjugates in the meanwhile.

The synthesis of three porphyrin-Schiff base conjugates was easy-operation and fast reaction, while their separation and purification was difficult by column chromatography because of the breakdown of C=N bond in acid medium. Therefore, the silica gel column was treated with alkaline triethylamine in advance to prevent the dissociation of the product and exhibit pretty good results.

3.2. Spectral properties of porphyrin-Schiff base conjugates

View Article Online
DOI: 10.1039/C6RA05682B

The UV-vis absorption spectra of **3a-3c** in dichloromethane solution showed one intense Soret band around 426 nm, followed by four weak Q-bands in the visible spectral region of 519-652 nm (**Fig 1**). Their spectra data were collected and summarized in **Table 1**. It can be seen that, the absorption peaks of porphyrins **3a-3c** exhibited no obvious wavelength difference and appeared slightly blue shifts compared with **TAPP**. This might be attributed to the chemical groups change from primary amine to Schiff base. The electronic effect from –N=C– and phenyl groups in porphyrin-Schiff base conjugates was similar to that of amino groups and phenyl groups in **TAPP** [29], and in the meanwhile the p-π conjugation between N atoms and porphyrin ring was weakened, which caused the blue shifts of Soret and Q band. Furthermore, the changes were almost the same, which indicated that the position of peripheral substituents was far from the porphyrin ring and had little effects on the distribution of electrons. Therefore, it did not produce noticeable effects upon the UV-vis absorption properties of **TAPP** [26].

The fluorescence emission spectra of **TAPP** and **3a-3c** in chloroform were obtained upon excitation at λ_{ex}=415nm, as shown in **Fig 2**. All compounds gave their emission spectra with different λ_{em} (**Table 1**) and the λ_{em} of the porphyrins conjugates were shorter than that of **TAPP**, which was owned to the effect of the peripheral substituents around the porphyrin chromophores. After changing from primary amine to Schiff base，the p-π conjugation between N atoms and porphyrin ring was changed to π–π conjugation and the decrease of π-electron cloud density of porphyrin ring resulted in a blue shift of λ_{em}. Comparing with **3b** and **3c,** the outermost substituted hydroxyl groups (–OH) in the compound **3a** had contribution to the electron cloud density of the conjugated porphyrin ring by electron donating effects, making the longer emission wavelength. The new weak emission peaks of the porphyrins conjugates around 712nm were appeared, while those peaks are absent on the spectra of **TAPP**, which might be attributed to electron transition from central H atom to the conjugated system of porphyrins [29, 30].

The vibrational spectroscopy can provide ample information about the structure of porphyrin. The tentative IR assignments of the **TAPP** and porphyrin-Schiff base

View Article Online
DOI: 10.1039/C6RA05682B

conjugates were reported in **Table 2**. The characteristic amino bands were found in **TAPP** at 1288 and 3443 cm^{-1}, while the characteristic amino bands were absent in the compounds **3a-3c**. However, three new bands ascribed to the stretching vibration of –C=N– at 1580, 1618 and 1628 cm^{-1} were observed in the IR spectra of compounds **3a-3c** respectively**,** which indicated that the expected porphyrin-Schiff base conjugates were successfully synthesized by the condensation of **TAPP** with the selected *p*-hydroxybenzaldehyde, 2-thenaldehyde and 2-pyridinecarboxaldehyde, respectively. A broad band appeared at 3423 cm^{-1} in the spectra of **3a** was assigned to ν_{O-H} of the phenolic. The band at 716 cm^{-1} was ascribed to ν_{C-S} of thiophene group of **3b**. The typical C-H peak of pyridine ring of **3c** was observed at 3053 and 800 cm^{-1}. In addition, all of the obtained compounds, including **TAPP** and porphyrin-Schiff base conjugates, showed a broad absorption band in the range 3445–3314 cm^{-1}, which was belonged to ν (NH) of porphyrin ring.

^{1}H NMR spectra of the compounds (**TAPP** and **3a-3c**) were recorded in d^6-DMSO and the peak assignment was summarized in (**Table 2**). As for **TAPP**, a sharp singlet was observed at 5.58 ppm and was assigned to H-atoms of NH_2 groups. Whereas, this amino proton signal was absent in the ^{1}H NMR spectra of compounds **3a-3c.** On the contrary, the azomethine protons (–CH=N–) appeared as a singlet at 8.83–9.18 ppm, which revealed that porphyrin-Schiff base derivatives were successfully synthesized by the condensation reaction. In addition, ^{1}H NMR spectra of the compound **3a** showed a peak at 10.22 ppm, which belonged to hydroxyl protons of the phenol [31]. Similarly, the multiplets for thiophene protons of **3b** and pyridyl protons of **3c** were detected in the range of 7.33–7.94 ppm and 7.63–8.09 ppm respectively[32]. Furthermore, the broad multiplet observed in the range 6.97–8.37 ppm for all of the obtained compounds was assigned to the aromatic protons. The ^{1}H NMR spectra of **TAPP** and the porphyrin-Schiff base derivatives all exhibited a weak singlet at approximately -2.83 ppm, which was the characteristic signal of the inner protons of porphyrin ring. The formations of all compounds were also confirmed by their mass spectral data given in the experimental section.

3.3 Photostability of compounds

View Article Online
DOI: 10.1039/C6RA05682B

The rate of photodegradation exhibit by a compound under light conditions is a very important parameter to assess when we consider their potential application as photosensitizer [33, 34]. In order to establish if porphyrin-Schiff base conjugates **3a-3c** could undergo photobleaching, we performed photostability studies in the same conditions of irradiation used for photocytotoxicity in the A431 cells (fluence rate 100 mW/cm $^{-2}$). The UV–vis and fluorescence emission spectra of each porphyrin (1 μM) were measured after different times of irradiation (0, 5, 10, 15, 20, 25, and 30 min). However, we observed minimal decay of absorption and emission intensity. As an example, the UV–vis and fluorescence emission spectra of porphyrin-Schiff base conjugates **3a** at different irradiation times are shown in **Fig 3**. The results point out that all compounds (**3a-3c**) showed high photostability under the conditions of the experiment, which is the desired property of a PDT photosensitizer.

3.4. Cytotoxicity assay

The cytotoxicity of the porphyrins **3a-3c** was evaluated by two kind of human skin cell lines, human keratinocyte HaCaT and epidermoid carcinoma A431. The cells seeded in well plates were treated with 10 μM of **3a**–**3c** solutions in the dark. As shown in **Fig 4**, the relative cell viability of A431 cells for **3a**–**3c** was in the range of 74.8%-75.5%, while that of HaCaT cells for **3a**–**3c** maintained from 86.5% to 109.8%. From the histogram of the cytotoxicity comparison in **Fig 4**, it was not hard to see that the cell viability of HaCaT and A431 cells was almost the same and maintained zzaround 92% and 82%, when cultured with **TAPP**, revealing that **TAPP** was almost harmless to both normal cells and cancer cells. However, porphyrins **3a–3c** showed higher cytotoxicity in dark to A431 cancer cells when compared with **TAPP**, especially for the porphyrin **3c**, which showed the highest cytotoxicity with the A431 cell viability of 74.8%. Conversely, negligible cytotoxicity was detected on HaCaT cells for compounds **3a–3c** with the cell viability of over 80% and even exceeded 100%. It was worth noting that **3b and 3c** was observed without cytotoxicity in dark for normal HaCaT cells and **3a** showed very slight cell damage. The cell survival histogram demonstrated that the synthesized porphyrin conjugates were more

View Article Online
DOI: 10.1039/C6RA05682B

effective to kill the cancerous A431 cells than the normal HaCaT cells at the concentration of 10 μM after 24 h of incubation and the antitumor activities of all of the porphyrin-Schiff base conjugates were evidently higher than that of **TAPP** with the same culture conditions. The results were attributed to the presence of the Schiff base, which showed conspicuous inhibitory to the growth of cancer cells.

3.5. Photodynamic effect

The in vitro phototoxicity studies were performed using A431 cells. The A431 cells adhered on the culture plate were incubated with porphyrins conjugates **3a-3c** solutions at the concentration of 10 μM for 24 h, respectively. After finishing the incubation, the samples were irradiated with blue light with the wavelength of 400 -450 nm, a fluence rate of 100 mW/cm^2 and light doses from 0 to 48 J/cm^2. Cell viability was determined by MTT assay. As shown in **Fig 5**, all of the tested compounds exhibited strong photocytotoxicity after exposure to the blue light for 0-480s, and the cell viability decreased dramatically with the increase of the light dose. The cell survival reduced sharply at the beginning of irradiation, and the decreasing tendency of cell viability became leveling off when the irradiation dose exceeded 12 J/cm^2.

The cells lines treated with **3a-3c** at different concentrations were irradiated with blue light for 360s. The compounds showed remarkable photodynamic effects at all concentrations. **Fig 6** showed the histogram of the cell viability at different compound concentrations, which indicated the viability of tumoral A431 cells reduced significantly with the increase of porphyrins concentration. The IC_{50} values, defined as the porphyrins concentration at which 50% of tumor cells were killed after the photoirradiation as compared to the control, were calculated based on the results of **Fig 6** and summarized in **Table 3.** From the IC_{50} values listed in **Table 3**, it was obvious that the conjugate **3a** was the most phototoxic under the above irradiation conditions with an IC_{50} of 0.57 μM, which was followed by **3b** with an IC_{50} of 1.19 μM and then **3c** with an IC_{50} of 1.31 μM. Notably, **3a** showed a 2.4 times enhanced photocytotoxicity compare to **TAPP**, which might be attributed to the attached phenolic group. The phenolic group is easily oxidized to benzoquinonyl group in

View Article Online
DOI: 10.1039/C6RA05682B

cellular metabolic pathway [35-37], which finally causes obvious cell damage.

3.6 Cellular uptake of porphyrin conjugates

It was a quite crucial question whether photosensitive compound could penetrate into the tumor cells for the therapeutic effect of PDT. Cellular uptake of porphyrins could be directly observed by fluorescence microscope without fluorescence labeling [38-40], for porphyrins uptaken by tumor cells would emit red fluorescence when being excitation. Based on the point, we could judge whether the porphyrins entered into the cells. In the fluorescence microscopic images **(**summarized in **Fig 7**), it was obvious that all the compounds could enter into the A431 cells causing intracellular fluorescence. The **3b** and **3c** samples displayed slightly brighter red fluorescence spots, while cells incubation with **3a** did not reveal enough fluorescence plots. These findings indicated that the conjugates **3a-3c** were different in cellular uptake and not in the nucleus. Furthermore, these intracellular levels of conjugates resulted in different photodynamic activities. Interestingly, the conjugate **3a** with the greatest photodynamic activity corresponded with the lowest intracellular uptake of all the conjugates tested.

4. Conclusion

In conclusion, three novel porphyrin conjugates **3a-3c** have been synthesized with excellent yields and their biological activities were evaluated by A431cells with a MTT assay. The conjugates **3b** and **3c** exhibited high selective inhibition against A431 cells in the absence of light. The result revealed that these conjugates could easily and selectively accumulate in tumor cells and had more cytotoxic effects on them. Incubation of A431 cells gave rise to an efficient cellular uptake of porphyrin conjugates, which was determined by fluorescence microscopy. The fluorescent image revealed that cells displayed an uptake of conjugates and appeared to be localized in the cytoplasm. The result was consistent with the strong photocytotoxic activity of porphyrin compounds after irradiation. The facts indicated that these porphyrin conjugates was a potential candidate of anticancer drugs in PDT, but their promising behavior needed further investigated investigation in vitro and in vivo experiments.

View Article Online
DOI: 10.1039/C6RA05682B

Acknowledgements

The authors acknowledge the research grant provided by the National Nature Science Foundation (21271148).

References

1 K. Chow, R. Sun, J. Lam et al, *Cancer Res*, 2010, **70**, 329-337.

2 B. Gustavsson, G. Carlsson, D. Machover, N. Petrelli et al, *Clinl Colorectal Canc*, 2015, **14**, 1-10.

3 J. Celli, B. Spring, I. Rizvi et al, *Chem. Rev*., 2010, **110**, 2795-2838.

4 M. Senge, M. Radomski, *Photodiagn. Photodyn.*, 2013, **10**, 1-16.

5 L. l. Hou, X.Y. Zhang, T.C. Pijper et al, *J. Am. Chem. Soc*., 2014, **136**, 910−913.

6 F. Hammerer, G. Garcia, S. Chen; P., *J. Org. Chem.*, 2014, **79**, 1406−1417.

7 M. G. Alvarez, E. I. Yslas, V. Rivarola, G. Mori, L. M. Penna, J. J. Silber, E. N. Durantini, *Molecules* , 2000, **5**, 379.

8 M. R. Detty, S. L. Gibson, S. J. Wagner, *J. Med. Chem.,* 2004, **47**, 3897.

9 U. cheffel, M. G. Pomper, *J. Nucl. Med.*, 2004, **45**, 1277.

10 J. Matsumoto, T. Shiragami, K. Hirakawa et al, *Int. J. Photoenergy,* 2015.

11 K. Davia, D. King, Y.L.Hong, S. Swavey, *Inorg. Chem. Commun.,* 2008, **11**, 584–586

12 S. Singh, A. Aggarwal, N. Bhupathiraju et al. *Chem. Rev.,* 2015, **115**, 10261-10306.

13 S. Yano, S. Hirohara, M. Obata et al, *J.Photoch. Photobio. C.,* 2011, **12**, 46-67.

14 M. Gomez-Tardajos, J. Pino-Pinto, C. Diaz-Soti et al, *Dyes. Pigments*, 2013, **99**, 759-770.

15 A. Fadda, R. El-mekawy, A. El-ahsfei et al, *J. Chem.*, 2013,1-11.

16 D.Kumar, K. Chandra Shekar, B. Mishra et al, *Bioorg. Med. Chem. Lett.*, 2013, **23**, 3221–3224.

17 M. Hranjec, K. Stacˇevic', S. K. Pavelic', P. Lucˇ in, K. Paveli, G. K. Zamola, *Eur. J. Med. Chem.*, 2011,**46**, 2274.

View Article Online
DOI: 10.1039/C6RA05682B

18 A. Abu-Dief, I. Mohamed, *Beni-Suef University Journal of Basic and Applied Sciences,* 2015, **4**, 119-133.

19 S. K. Bharti, G. Nath, R. Tilak, S. K. Singh, *Eur. J. Med. Chem*.,2010, **45**, 651.

20 M. Laranjo, A. Serra, M. Abrantes et al, *Photodiagn photodyn*., 2013, **10**, 51-61.

21 L. Q. Luan, L. L. Ding, W. J. Zhang et al, *Bioorg. Med. Chem. Lett.*, 2013, **23**, 3775-3779.

22 S.P. Songca, B. Mbatha, *J. Pharm. Pharmacol.*, 2000, **52**, 1361-1367.

23 G. Szalóki, A. Pantzou, K. Prousis et al, *Bioorg. Med. Chem.,* 2014, **22**, 6980–6988.

24 Choudhary, M. I.; Alam, M. S.; Atta-ur-Rahman; Yousuf, S.; Wu, Y.-C.; Lin, A.-S.; Shaheen, F, *Steroids* 2011, **76**, 1554

25 A. Bettelheim, B. A. White, S. A. Raybuck et al, *Inorg. Chem.,* 1987, **26**, 1009-1017

26 H.M.Wanga, J.Q. Jiang b, J.H. Xiaoa, R.L. Gaoa, F.Y. Linb, X.Y. Liub, *Chem-Biol. Interact.,* 2008, **172**, 154–158

27 J. L. Merlin, S. Azzi, D. Lignon, C. Ramacci, N. Zeghari, F. Guillemin, *Eur. J. Cancer*, 1992, **28**, 1452.

28 E. Fischer-Fodor, N. Moldovan, P. Virag, O. Soritau, I. Brie, P. Lönnecke, et al, *Dalton Trans*, 2008, **45**, 6393-400.

29 Y. H. Wu, L. Chen, J. Yu, S.L. Tong, Y. Yan, *Dyes. Pigments*, 2013, **97**, 423-428.

30 M. Uttamlal, A. S. Holmes-Smith, *Chem. Phys. Lett.*, 2008, **454**, 223-8.

31 S. Amer, N.Wakiel , H.Ghamry, *J. Mol. Struct.*, 2013, **1049**,326–335.

32 A. Bhat, F. Athar, R. Van Zyl, C.T. Chen, A. Amir, *Chem. Biodivers.*, 2008, **5**, 764-776.

[33] V.V. Serra, A. Zamarrón, M. A. F. Faustino, M. C. Cruz, F. Sanz-rodríguez, et al, *Bioorg. Med. Chem*., 2010, **18**, 6170–6178.

[34] Y. Ko, K. J. Yun, M.S. Kang, J. Park, J. H. Shin, et al, *Bioorg. Med. Chem. Lett*., 2007, **17**, 2789-2794.

[35] S. B. Colbran, S. T. Lee, D. G. Lonnon, F. J. D. Maharaj, A. M. McDonagh, K. A. Walker, R. D.Young, *Organometallics*. 2006, **25**, 2216.

View Article Online
DOI: 10.1039/C6RA05682B

[36] F. M.F. Roleira, E.J. Tavares-da-Silva, C.L. Varela, S. C. Costa, F. Borges, et al, *Food Chem.,* 2015*,* **183**, 235-258.

[37] X.L. Liu, M.M. Zhao, K.G. Wu, X.H. Chai, H.G. Yu, Z.H. Tao, J. H. Wang, *Food Chem.,* 2012, **131**, 685-690.

38 F. Schmitt, J. Freudenreich, N. Barry et al, *J. Am. Chem. Soc*., 2012, **134**, 754-757.

39 A. Gorman, J. Killoran, C. OShea, T.Kenna, W.M. Gallagher, D.F. OShea, *J. Am. Chem. Soc.*, 2004, **126**, 10619-10631.

40 Y. J. Ko, K. J. Yun, M.S. Kang, J. Park, K.T. Lee, S.B. Park, J.H. Shin, *Bioorg. Med. Chem. Lett.,* 2007, **17**, 2789-94.

FIGURES AND SCHEME CAPTIONS

Table 1. Optical data for **TAPP** and **3a-3c** ($CHCl_3$, 25^o C)

Table 2 ^{1}H-NMR and IR spectral bands of **TAPP and 3a-3c**

Table 3. IC_{50} value of **TAPP** and **3a–3c for** A431 cells

Scheme 1. Synthetic routes of **TAPP** and **3a–3c**

Fig 1 UV-vis absorption spectra of **TAPP** and **3a–3c**

Fig 2 The fluorescence spectra of **TAPP** and **3a–3c**. Concentrations of the porphyrins were 1×10^{-6} mol/L in $CHCl_3$

Fig 3 UV-Vis absorbance spectra (A) and Emission spectra (B) of porphyrin **3a** after different times of irradiation

Fig 4 Cytotoxicity of **TAPP** and **3a–3c** on A431 cells and normal skin cells

Fig 5 Relative cell viability of A431 cells irradiated with light doses from 0 to 48 J.cm^{-2}

Fig 6 Relative cell viability of A431 cells at different concentrations of porphyrins **TAPP** and **3a–3c**

Fig 7 Fluorescence microscopy of A431 cells incubated with **TAPP** and **3a-3c** (10μM, 24h) (Left) white light and (Right) fluorescence

View Article Online
DOI: 10.1039/C6RA05682B

Table 1 Photophysical data of **TAPP and 3a-3c** ($CHCl_3$, 25° C)

Compounds	Soret band (nm)	Q bands (nm)	λem(nm)
TAPP	428.0	523.0, 563.5, 598.0, 656.0	665
3a	426.5	520.5, 559.0, 594.5, 652.0	657, 711
3b	426.5	520.0, 557.0, 594.0, 650.5	655, 712
3c	425.5	519.5, 557.0, 593.5, 651.0	655, 712

Table 2 ^{1}H-NMR and IR spectral bands of **TAPP and 3a-3c**

Comp.	^{1}H-NMR spectra (ppm)				IR spectra (cm^{-1})		
	$\delta_{innerNH}$	$\delta_{\beta\text{-}H}$	$\delta_{Ar\text{-}H}$	δ_{NH} or $\delta_{CH=N}$	ν_{NH}	$\nu_{C=N}$(imine)	$\nu_{C=N}$(ring)
TAPP	-2.74	8.89	7.01-7.86	5.58	3375	--	1465
3a	-2.83	8.92	6.97-8.22	8.83	3314	1580	1468
3b	-2.84	8.94	8.22-8.26	9.18	3445	1618	1425
3c	-2.83	8.94	7.82-8.37	8.83	3437	1628	1470

Table 3 IC_{50} value of **TAPP** and **3a–3c for** A431 cells

Compounds	IC_{50}(μM)
TAPP	1.36
3a	0.57
3b	1.19
3c	1.31

View Article Online
DOI: 10.1039/C6RA05682B

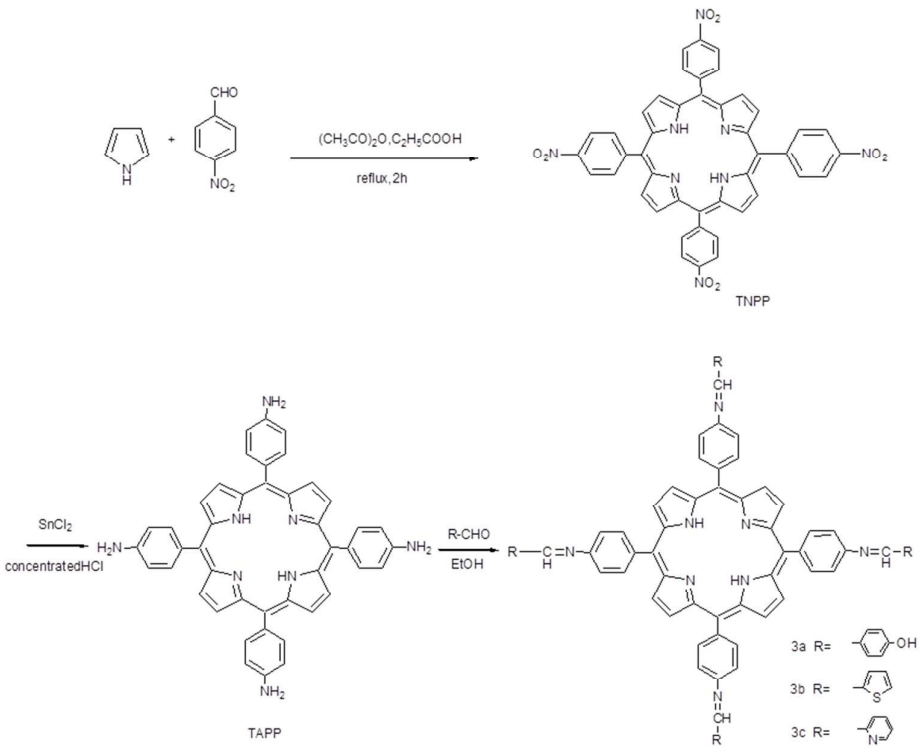

Scheme 1 Synthetic routes of **TAPP** and **3a–3c**

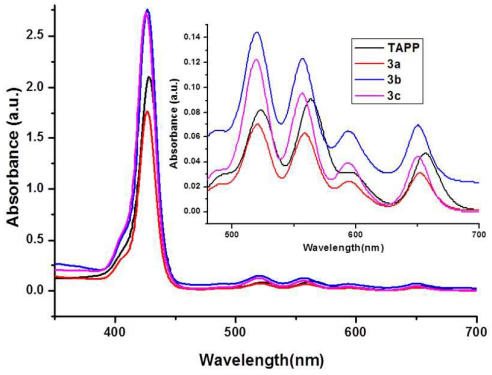

Fig 1 UV-vis absorption spectra of **TAPP** and **3a–3c**

View Article Online
DOI: 10.1039/C6RA05682B

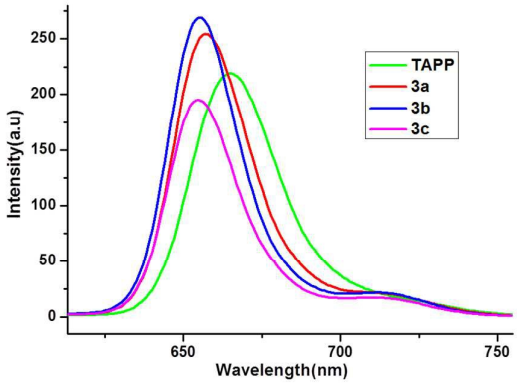

Fig 2 The fluorescence spectra of **TAPP** and **3a-3c**. Concentrations of the porphyrins were 1×10^{-6} mol/L in $CHCl_3$

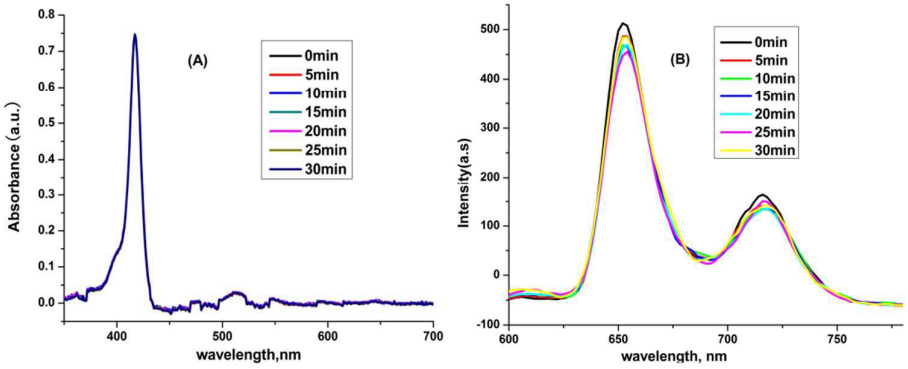

Fig 3 UV-Vis absorbance spectra (A) and Emission spectra (B) of porphyrin **3a** after different times of irradiation

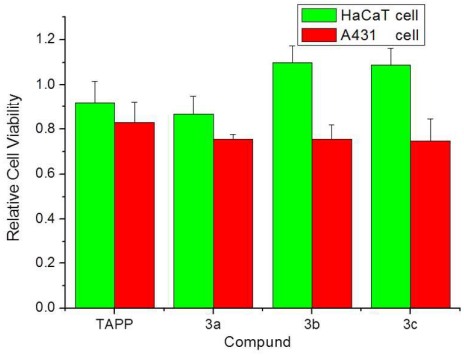

Fig 4 Cytotoxicity of **TAPP** and **3a**–**3c** on A431 cells and normal skin cells

View Article Online
DOI: 10.1039/C6RA05682B

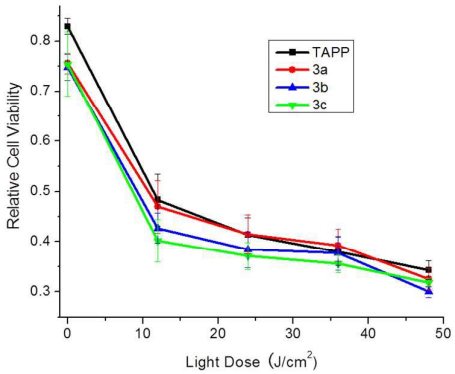

Fig 5 Relative cell viability of A431 cells irradiated with light doses from 0 to 48 J.cm^{-2}

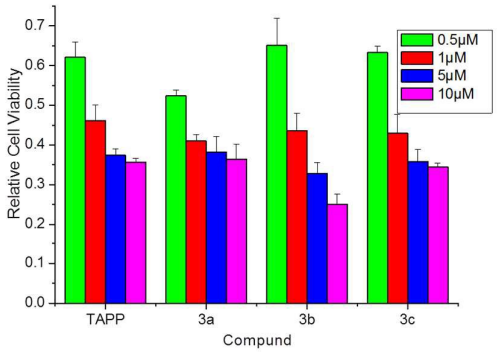

Fig 6 Relative cell viability of A431 cells at different concentrations of porphyrins **TAPP** and **3a–3c**

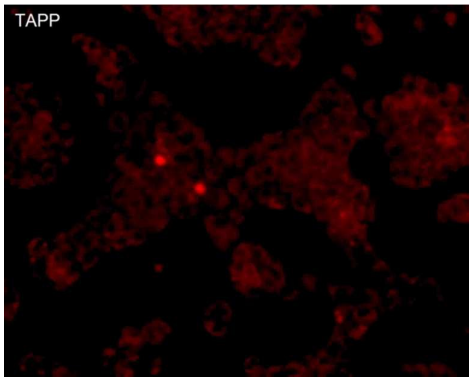

View Article Online
DOI: 10.1039/C6RA05682B

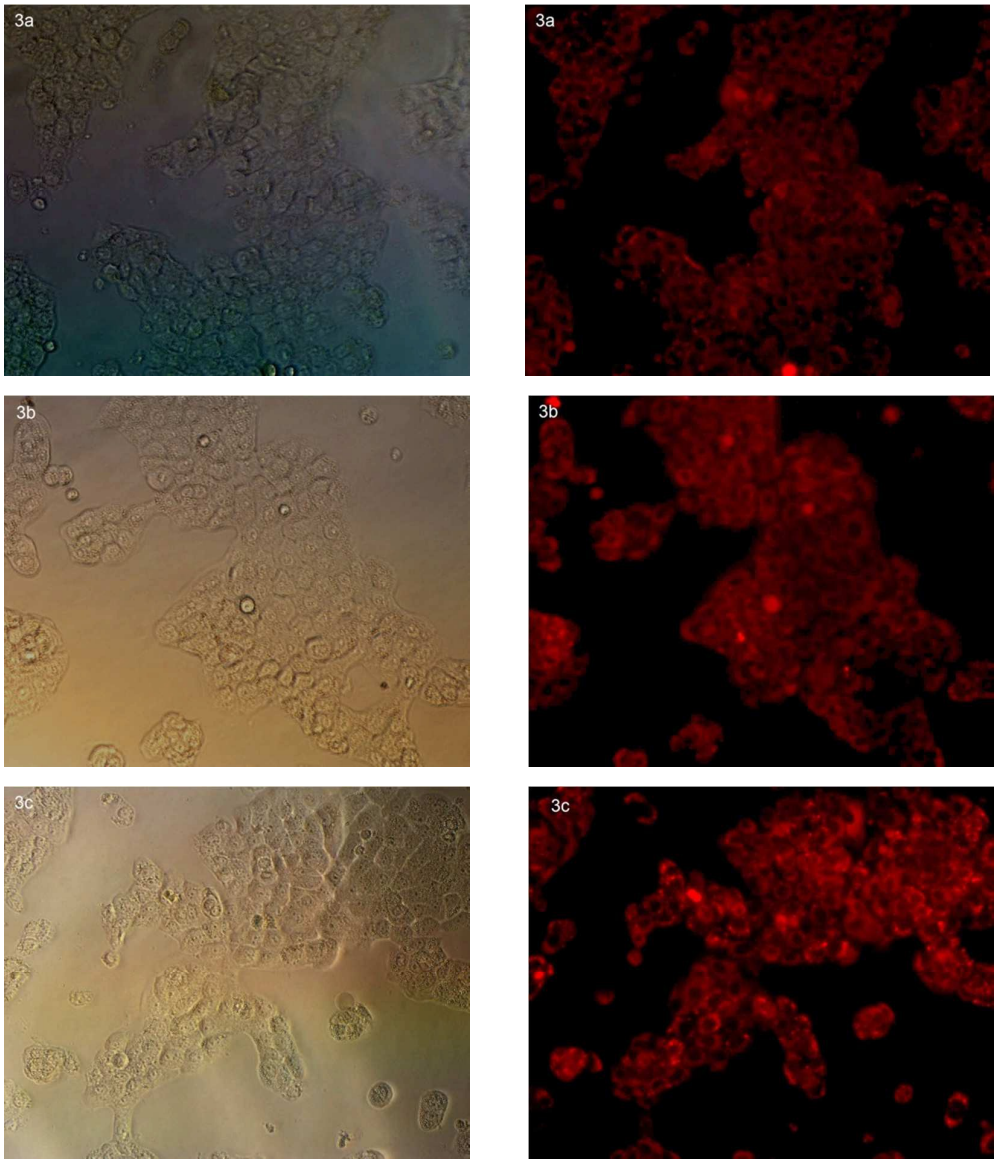

Fig 7 Fluorescence microscopy of A431 cells incubated with **TAPP** and **3a-3c** (10μM, 24h) (Left) white light and (Right) fluorescence

View Article Online
DOI: 10.1039/C6RA05682B

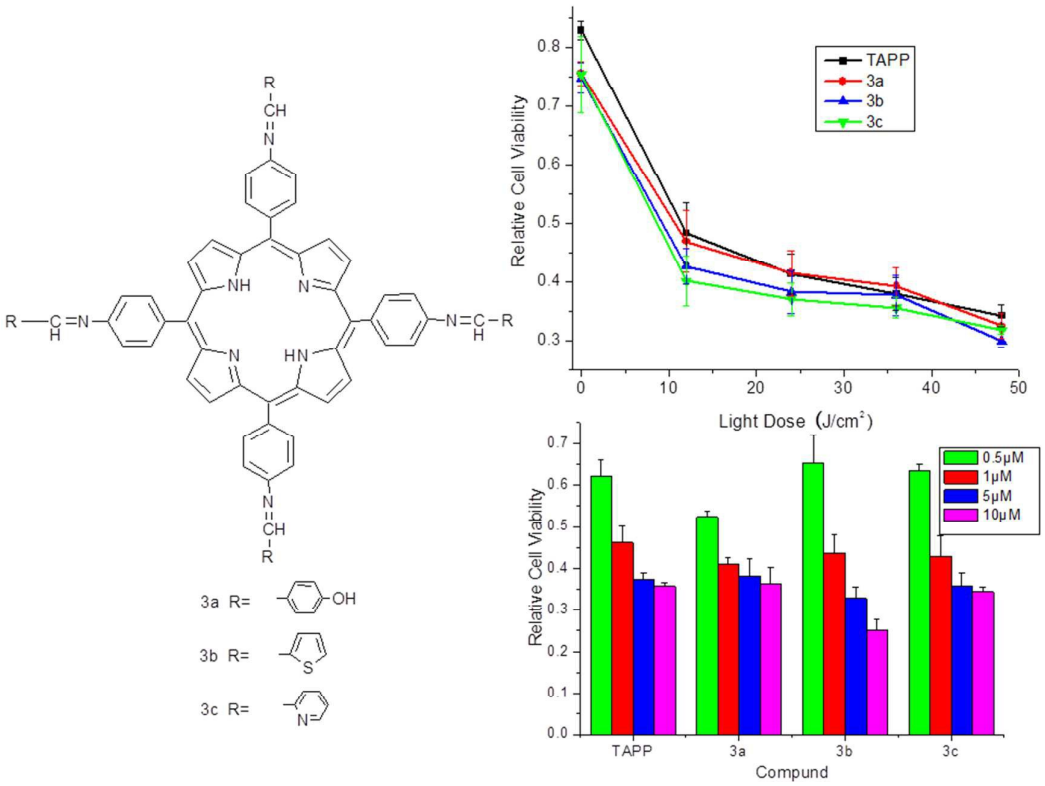

Three novel porphyrin-schiff base conjugates were synthesized and characterized. Their phototoxic activities were improved after irradiation and increased significantly with the increase of doses against A431 cells.